Climate Services 33 (2024) 100434

Contents lists available at ScienceDirect

Climate Services

journal homepage: www.elsevier.com/locate/cliser

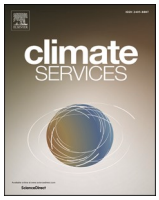

Original research article

Increasing the prospective capacity of global crop and rangeland monitoring with phenology tailored seasonal precipitation forecasts

Michele Meroni [a,1], Petar Vojnović [b,1], Matteo Zampieri [c,d], Stefano Materia [e,f], Felix Rembold [c,*], Oliver Kipkogei [g], Andrea Toreti [c]

[a] Seidor Consulting, Barcelona, Spain
[b] Fincons, Milan, Italy
[c] European Commission, Joint Research Centre (JRC), Ispra, Italy
[d] King Abdullah University of Science and Technology (KAUST), Thuwal, Saudi Arabia
[e] EuroMediterranean Center on Climate Change (CMCC), Bologna, Italy
[f] Barcelona Supercomputing Center (BSC), Barcellona, Spain
[g] IGAD Climate Prediction and Applications Centre (ICPAC), Nairobi, Kenya

ARTICLE INFO

Keywords:
Drought
Agriculture
Early warning systems
Seasonal climate forecast
Crop and rangeland phenology
Food security

ABSTRACT

Droughts are more and more often a limiting factor to agricultural production and can have severe negative effects on food security in vulnerable countries. Global agriculture early warning systems monitor agriculture in near real-time by analyzing meteorological data (e.g. precipitation and temperature) and optical remote sensing data as proxy vegetation health to detect possible negative anomalies and trigger warnings. Seasonal climate forecast can add a predictive component and inform about upcoming precipitation deficits, thus allowing anticipation and improved planning of response actions. Here, we propose a scheme to adapt the standard precipitation forecast from the seasonal Copernicus Climate Change Service multi-system to crop and rangeland phenology, making them suitable for agricultural early warning. Precipitation forecasts are first elaborated into tercile maps showing the probability of the most likely tercile (i.e. drier than normal, normal, wetter than normal) and associated skills of all possible monthly periods combinations included in the six months forecasting horizon. Afterwards, agronomically relevant tercile maps are produced for the closest season in time at any location. These maps are obtained by mosaicking the forecasts for the appropriate growing season period at each grid cell. The resulting map shows the tercile probability for the remaining part of the ongoing growing season (if any at time of analysis) or the probability of the next upcoming season (if in between growing season at time of analysis). The proposed methodology offers a precipitation seasonal forecast product ready to use by agricultural analysts and directly ingestible by automatic warning systems.

Practical implications

Global agriculture early warning systems (e.g. the European Commission – Joint Research Centre Anomaly hotSpot of Agricultural Production, ASAP, https://agricultural-production-hotspots.ec.europa.eu; the FAO Agriculture Stress Index System, ASIS, https://www.fao.org/giews/earthobservation/asis/index_1.jsp?lang=en; the World Food Program Vulnerability Analysis and Mapping (VAM) Climate Explorer, https://dataviz.vam.wfp.org/version2/climate-explorer) monitor in near real-time the development and status of agricultural land using meteorological and remote sensing data to detect deviations from normal conditions at the time of analysis. In this contribution we move one step further to the monitoring of current agricultural situation by providing information on the future precipitation, a major driver of agricultural production in food insecure countries where droughts can have devastating impact on livelihoods. Seasonal precipitation forecasts gathered from the Copernicus C3S multi-system Seasonal Climate Forecast are tailored to match the temporal dynamics of crops and rangeland using the remote sensing

* Corresponding author.
E-mail address: felix.rembold@ec.europa.eu (F. Rembold).
[1] Under contract with the European Commission, JRC, Ispra, Italy.

https://doi.org/10.1016/j.cliser.2023.100434
Received 30 March 2023; Received in revised form 13 December 2023; Accepted 20 December 2023
Available online 11 January 2024

derived Land Surface Phenology information of the ASAP early warning system. By extracting precipitation forecast for the relevant agronomic period at the ASAP grid cell level (1 km spatial resolution) and mosaicking them globally, we produce precipitation probability maps that inform the user on the likely precipitation forecasted for the remaining part of the agricultural season (where a season is ongoing at the time of analysis) or for the upcoming season (where the timing of analysis falls between the seasons). In contrast to standard tercile maps referring to a fixed time span (e.g. next three months), this information, together with its reliability from mosaicked skill information, provides a direct overview of the precipitation probability relevant to agriculture and can be ingested in the automatic processing of ASAP to trigger warnings of future precipitation deficit.

Data availability

Data will be made available on request.

1. Introduction

Climate variability and extremes, together with conflicts and economic slowdowns and downturns (recently exacerbated by socio-economic impacts of COVID-19 pandemic and Russia's war against Ukraine) are major drivers of food insecurity and malnutrition. They are key drivers behind the recent rises in global hunger and among the leading causes of severe food crises (FAO et al., 2018; Food Security Information Network et al., 2022). Extremes have been increasing in both frequency and intensity, and are occurring more frequently as concurrent and compound events (FAO et al., 2021, IPCC, 2021). There is high confidence that increasing weather and climate extreme events have exposed millions of people to acute food insecurity and reduced water security, with the largest impacts observed in many locations in Africa, Asia, Central and South America, Small Islands and the Arctic (IPCC, 2022). Recurrent droughts across large parts of Africa occurred in 2021 (World Meteorological Organization, 2022a) and 2022 (World Meteorological Organization, 2022b) threatening food security in the Horn of Africa (e.g. ICPAC et al., 2022) and in parts of Southern Africa such as Madagascar.

Global early warning systems using meteorological and remote sensing data have been developed by both national and international institutions and provide information on potential food production anomalies resulting from climate shocks (Fritz et al., 2019; Nakalembe et al., 2021). Several of these systems are collaborating under the coordination of global networks such as GEOGLAM (Group on Earth Observation Global Agricultural Monitoring) which specifically produces the monthly Crop Monitor for Early Warning bulletins in countries at risk of food insecurity (Becker-Reshef et al., 2020). The European Commission's Joint Research Centre contributes to this network through the ASAP (Anomaly hotSpot of Agricultural Production) online decision support system focusing on agricultural production anomalies for crops and rangelands (Rembold et al., 2019).

The Hotspot Assessment of ASAP (https://agricultural-production-hotspots.ec.europa.eu) provides monthly identification of countries with agricultural production problems and summary narratives that synthesize, in non-technical terms, the analysis of anomalies of the weather- and remote sensing-derived indicators during the previous 30 days at national level. The identification of the hotspots builds on the automatic warning classification scheme of the Warning Explorer (https://agricultural-production-hotspots.ec.europa.eu/wexplorer/), an advanced web-GIS with a dashboard for the visualization of indicators' statistics. Automatic warnings at GAUL1 or GAUL2 level (FAO Global Administrative Unit Layers) are generated every 10 days, targeting croplands and rangelands. Warnings are based on the crop (or rangeland) area that exceeds a critical anomaly threshold of selected indicators (Meroni et al., 2019): the normalized difference vegetation index (NDVI) over the growing season as a proxy of biomass production; the Standardized Precipitation Index over a three-month time scale (SPI3, World Meteorological Organization, 2012); and the Water Satisfaction Index (WSI), an indicator of crop (or rangeland) performances based on the water availability to the plants during the growing season obtained from a soil water balance model (Boogaard et al., 2018). Agriculture monitoring analysts can use the Warning Explorer to browse the maps of various indicators and inspect summary statistics and temporal profiles of various indicators aggregated at the sub-national administrative level. The variables available are not limited to those used for the warning classification scheme but include various others relevant for crop and rangeland monitoring (e.g. temperature, solar radiation, soil moisture). Warning Explorer data are global, free and open.

Users of early warning decision support systems need simple and easy-to-obtain knowledge for informed evaluation of upcoming drought impacts. It is thus crucial to translate the massive amount of climate data and information available into meaningful and customized tools and services in a way that can be used by the largest audience possible (Giuliani et al., 2017, Materia et al., 2020). For instance, when focusing on crop monitoring, meteorological and remote sensing biomass proxy data over non-cropped area or at times of the year when crops are not actually growing can be misleading. For this reason ASAP focuses only on indicators in specific areas and time periods that are agronomically relevant. This means monitoring only areas where crops (or rangeland) are present and at times when they are expected to be growing. Warnings are triggered only if anomalies of the various indicators used in the warning system occur in cropland (or rangeland) areas as defined by a crop (or rangeland) mask and at times when (on climatological average) there is an active growing season. To define the average growing season period, ASAP uses the satellite-derived climatological land surface phenology (De Beurs and Henebry, 2005).

Although NDVI anomalies can be originated by different threats to vegetation (e.g. droughts, floods, pests), ASAP focuses mainly on water availability and it is essentially an agricultural drought monitoring system. Thanks to such a system, users can monitor near real-time the crops or rangelands evolution up to the current time.

In order to provide probabilistic information on possible future crop development, we included seasonal precipitation forecasts gathered from the Copernicus C3S multi-system Seasonal Climate Forecast (SCF). Here, we focus on precipitation as the most important driver of drought phenomena and more generally of crop productivity.

Dynamical seasonal climate forecasts provide predictions at monthly-to-seasonal time scales, based on the assumption that large-scale and long-lasting anomalies, particularly in the ocean and land surface, will convey predictive skill (e.g. Barnston et al., 1994). The seasonal climate forecasts of the Copernicus Climate Change Service (C3S) are produced by several research centers, and homogenized in terms of resolution and length of the hindcast period to ease the generation of a multi-model.[2] A simple combination of the prediction systems is not necessarily the best choice (Hemri et al., 2020), although often more complicated ways of combining different systems did not generate an increase of forecast quality (Mishra et al., 2019). Yet, how to best combine the multi-model forecast is still a matter of debate (Hemri et al., 2020).

Seasonal precipitation skill is generally poorer than other more persisting and less erratic variables, such as land and ocean surface temperatures. Errors may be due to a poor prediction of the predictability drivers, wrong links between the large and local scales, and

[2] https://confluence.ecmwf.int/display/CKB/C3S+Seasonal+Forecasts.

model errors in the representation of local processes (MacLeod, 2019). However, seasonal precipitation skill is often adequate in the Tropics and other regions characterized by a strong teleconnection with ENSO, which is well represented by coupled climate models (Lenssen et al., 2020). Product skill can be further enhanced by aggregating or smoothing the forecasts, but specifically for precipitation, skill improves only scarcely and just with temporal aggregation, since spatial smoothing is often detrimental for variables that are spatially highly inhomogeneous (Kharin et al., 2017).

C3S delivers seasonal forecast data every month. Aggregated forecast maps over a 3-month period are available in the form of anomalies from the models' climatological mean for different variables, including precipitation. These maps do not necessarily coincide with the spatial and temporal domain relevant for crop or rangeland monitoring, and leave the user with the challenge of understanding where anomalies overlap with land covered by crops and rangelands, and whether the forecast horizon they are spanning is relevant (e.g. does it overlap with a growing season? does it cover it all?). Furthermore, information about forecast skill is missing in C3S, making it difficult for analysts to have an indication about the reliability of the forecast at different times and over different areas.

To facilitate the use and uptake of SCF for the agricultural sector, this manuscript focuses on the integration and tailoring of precipitation SCF to cropland and rangeland phenology used in the ASAP system. To our knowledge, this represents the first attempt to adapt seasonal climate forecasts to agricultural seasonality for their use in an automatic early warning system.

2. Data

The integration of seasonal forecast into the ASAP system aims at presenting forecasts only where and when they are relevant for cropland and rangeland monitoring and thus exploits three main building blocks: the ASAP cropland and rangeland masks, the satellite-derived land surface phenology of ASAP and precipitation forecast from the Copernicus C3S multi-system.

2.1. ASAP cropland and rangeland masks

The ASAP global early warning system, as other systems (Fritz et al., 2019), relies on static cropland and rangeland masks to define the area where anomalies of various indicators can be considered relevant for agricultural early warning. Masks are available at the ASAP global spatial grid reference system (currently 1 km resolution) as Area Fraction Images (AFIs): cropland and rangeland area are identified by the percentage of the grid cell area occupied by the given target, either cropland or rangeland. AFIs enable computation of administrative level statistics of meteorological and remote sensing data weighted by fractional cover.

The ASAP cropland and rangeland masks are derived by combining different land cover datasets, using criteria such as spatial resolution and time of production into one globally optimized layer. In the translation of the legends of the various datasets we adopted the following definitions of croplands and rangelands. Cropland is defined as the land used for cultivation of crops, encompassing both total areas under arable land and permanent crops. Grassland is defined according to FAO-GLCshare. Thus, grasslands include any geographic area dominated by natural herbaceous plants with a cover of 10 % or more, irrespective of different human and/or agricultural activities, such as grazing. Woody plants (tree and/or shrubs) can be present if cover is less than 10 %. For further details on the masks derivation from multiple land cover products see Meroni et al.(2019) and Pérez-Hoyos et al., (2020,2017).

2.2. ASAP phenology

To define the mean growing season period per pixel we use the satellite-derived land surface phenology computed on the long-term (2002–2016) average of 10-day NDVI Moderate Resolution Imaging Spectroradiometer (MODIS) data at 1 km spatial resolution processed according to Klisch and Atzberger (2016) for optimal noise removal in near real-time applications. Land surface phenology is computed on NDVI temporal trajectory curves using an approach based on thresholds on the green-up and decay phases as described in White et al. (1997).

The following key parameters are retrieved for each grid cell: number of growing seasons per year (i.e. one or two); start of season (SOS, i.e. the time when NDVI rises above 25 % of the ascending amplitude of the seasonal profile); time of maximum NDVI (TOM); start of senescence period (SEN, when NDVI drops below 75 % of the descending amplitude); and end of the season (EOS, when NDVI drops below 35 %).

With this information it is then possible to determine, at any time of analysis, if a pixel is expected to be "active" (i.e. in the period of average growing season) and to compute the progress of the season and the expected phenological stage. The progress of the season is the percentage of the length of the growing season (i.e., EOS minus SOS) that has passed at the time of analysis. The period between SOS and TOM is referred to as phenological stage "expansion", the one between TOM and SEN as "maturation", and the one between SEN and EOS as "senescence".

2.3. Precipitation forecasts from C3S

We use single-level total precipitation forecast coming from the seasonal multi-system made available on the Copernicus Data Store.[3] Data includes forecasts created in real-time (since 2017) and retrospective forecasts (hindcasts) initialized at equivalent intervals during the period 1993–2016. Forecasts are global and at 1° x 1° spatial resolution. We use precipitation forecasts aggregated on a monthly temporal resolution with a 6-month forecasting horizon. Real-time forecasts are released once per month on the 13th at 12 UTC.

In particular, we make use of the following six forecast systems: ECMWF, UKMO, Meteo-France, DWD, CMCC, and NCEP (Table 1 for the number of ensemble members). JMA and ECCC systems are not included because at the time the study started, JMA was available with a reduced number of ensemble members (10) and a reduced spatial resolution (2.5°) while ECCC was not yet available in C3S.

Each system has its own models and/or parameterization and uses slightly different initialization strategies, leading to different model's biases, uncertainties, and thus realizations. Combining the output from a number of models enables a more realistic representation of the uncertainties due to model error and on average, more skillful than forecasts from the best of the individual models.[4]

Table 1
Number of ensemble members per forecasting system.

Forecast system	Ensemble size	
	Forecast	Hindcast
ECMWF	51	25
UKMO	56	28
Meteo-France	51	25
DWD	50	30
CMCC	50	40
NCEP	120	28
Total	*378*	*176*

[3] https://cds.climate.copernicus.eu/cdsapp#!/dataset/seasonal-monthly-single-levels?tab=overview.

[4] https://confluence.ecmwf.int/display/CKB/Seasonal+forecasts+and+the+Copernicus+Climate+Change+Service.

2.4. Observational precipitation

We used the Rainfall Estimates from Rain Gauge and Satellite Observations (CHIRPS) version 2 (Funk et al., 2015) as observational reference dataset. CHIRPS data are remapped from the original 0.05° spatial resolution to the 1° grid of the seasonal forecast model using a conservative method (Chen and Knutson, 2008; Jones, 1999), in order to be compatible with the seasonal forecast data.

3. Methods

As a first step for adapting precipitation forecast to agricultural phenology, we compute tercile maps (Section 3.1) and their skills (Section 3.2) for all the possible starting and ending months within the forecasting horizon. This information is then mosaicked spatially using crop and rangeland phenology at 1 km spatial resolution (Section 3.3).

3.1. Seasonal forecast tercile maps

We map precipitation forecasts as the probability of the most likely tercile predicted by the entire set of ensemble members coming from the six seasonal forecast systems considered.

Terciles are computed scrutinizing the ensemble set of the forecasts made in the past (hindcasts), and represent the three 33rd percentiles (pct) of the lowest, the highest and in between (normal) precipitation accumulated throughout the lead time of interest, for each grid cell in the hindcasts. Having 24 years of hindcasts (1993–2016) and taking the ECMWF forecast system as an example, each grid cell always contains 600 values of precipitation forecasted in the past (24 years × 25 ensemble members). The lowest 200 values (precipitation ≤ 33rd pct) are included in the lower tercile and represent below normal precipitation, the highest 200 values (precipitation ≥ 67th pct) are included in the higher tercile and represent above normal precipitation, the values in between (33rd pct < precipitation ≤ 66th pct) represents normal precipitation. Thus, each category (tercile) is characterized by one third probability of occurrence.

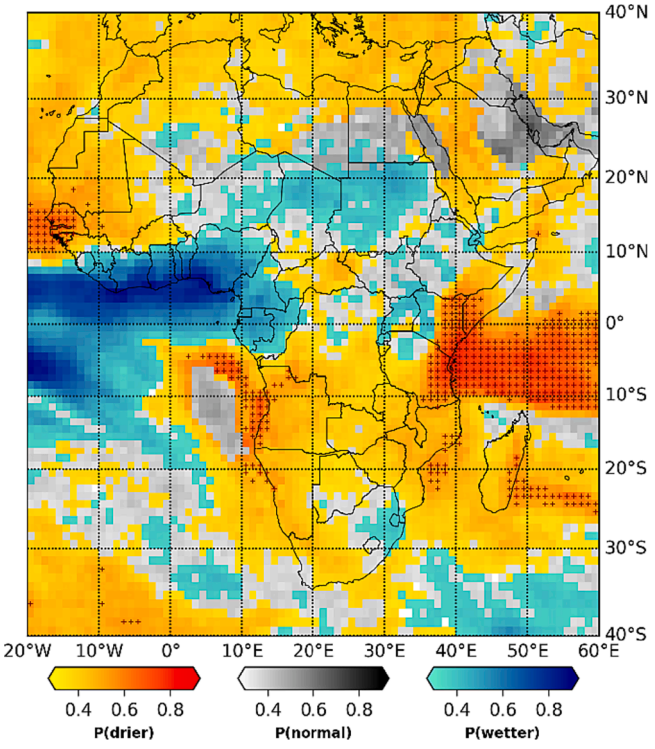

Fig. 1. Example of tercile map over the African continent for the seasonal forecast of August 2021 referring to the period 01/08/2021 – 31/10/2021. The "+" sign indicated a relatively high probability (i.e. at least 32%) of precipitation equal or below the 16th percentile (that is, below one standard deviation).

Terciles maps (see Fig. 1 for an example over the African continent) are here computed using all 378 forecast members (Table 1) by counting how many of the ensemble members predict a precipitation anomaly within each of the terciles calculated in the hindcasts. That is, for each tercile, we sum the number of members of all the forecast systems falling in that tercile. Then we divide such number of occurrences by the total number of members, resulting in a probability of each tercile. Terciles maps have a 100 km grid cell and show the probability of the most likely category (drier than normal, normal, wetter than normal), that is the category predicted by the relative majority of ensemble members.

As an example, consider the following case. There are a total of 378 forecast members, 200 of them predict precipitation below normal (falling in first tercile), 100 predict precipitation within the norm and 78 predict precipitation above normal. The corresponding grid cell will be yellow-orange, indicating a 52.9 % probability (200 members out of 378) for precipitation below normal. The sum of each of these probabilities totals 100 %, and only the information about the category having the highest forecast probability is mapped.

In addition, in case the forecast indicates a relatively high probability (i.e. at least 32 %) of precipitation equal or below the 16th percentile (that is below the standard deviation), a "+" sign is drawn on the grid cell. The system is in fact communicating higher confidence in drier than usual conditions, as there is (at least) a 32 % percent chance for a precipitation anomaly that only occurred 16 % of the times in the past.

Tercile maps can be considered a standard for visualizing seasonal forecasts. For example, tercile maps for a period referring to the three months after the forecasting time are available in C3S.[5] Here we extend this computation to all possible monthly aggregations that can be formed with the six monthly forecasts issued every month, to allow further processing needed to produce phenology adapted tercile maps. As an intermediate product, this suite of maps can be useful to an analyst interested in precipitation forecasts over a specific period of the year.

3.2. Skills

The skill assesses the gain in forecast quality with respect to a forecast benchmark (Hargreaves, 2010), which usually consists of the observed climatology (Wilks, 2011). Skill provides an essential indication for the assessment of the forecast value, utility and reliability to be delivered to the users (Crochemore et al., 2023).

Forecast skills are computed comparing hindcasts with CHIRPS precipitation data, considered here as observational reference dataset, to derive the ranked probability skill score (RPSS, Wilks, 2011).

The ranked probability score (RPS) is a measure of how good multiple category frequencies (in this case tercile frequencies) are in matching observed outcomes, being 1 if the forecasted event occurs, and 0 if the event does not occur. However, to be sensitive to the distance between the forecasted and observed event in the case of ranked multicategory events, the errors are computed with respect to the cumulative probabilities in the forecast and observation vectors.

Let J be the number of event categories (here 3) and P the probability vector of the forecast. For instance, if the forecast is 20 % chance of dry, 30 % chance of near-normal, and 50 % chance of wet, then the P vector would have the following 3 components: $p_1 = 0.2$, $p_2 = 0.3$, and $p_3 = 0.5$. Similarly, the observation vector O has three components being all 0 but one corresponding to the event that occurs, for instance in the wet category: $o_1 = 0$, $o_2 = 0$, and $o_3 = 1$.

The cumulative forecast and observation vectors, denoted P_m and O_m, are then defined as:

[5] https://climate.copernicus.eu/charts/c3s_seasonal/.

$$P_m = \sum_{j=1}^{m} p_j, \quad m = 1, \cdots, J;$$

$$O_m = \sum_{j=1}^{m} o_j, \quad m = 1, \cdots, J;$$

In terms of the foregoing hypothetical example, $P_1 = p_1 = 0.2$; $P_2 = p_1 + p_2 = 0.5$; $P_3 = p_1 + p_2 + p_3 = 1$; and $O_1 = o_1 = 0$; $O_2 = o_1 + o_2 = 0$; $O_3 = o_1 + o_2 + o_3 = 1$. The ranked probability score is the sum of squared differences between the components of the cumulative forecast and observation vectors:

$$RPS = \sum_{m=1}^{J} (P_m - O_m)^2$$

A perfect forecast would assign all the probability to the single p_j corresponding to the event that subsequently occurs, so RPS = 0. Forecasts that are less than perfect receive scores that are positive numbers, so the higher the RPS. The largest RPS value are obtained when forecast probability is concentrated on one extreme tercile (first or third) and the opposite extreme tercile is observed (RPS = 2). Jointly evaluating a collection of n forecasts using the ranked probability score requires averaging the RPS values for each forecast-event pair:

$$< RPS >= \frac{1}{n} \sum_{k=1}^{n} RPS_k$$

For the skills of forecasts issued on month M and lead time L, the n forecasts are here represented by the forecasts issued in month M with lead time L each year during the hindcasts periods (1993–2016), thus n is constant and equal to 24.

The ranked probability skill score (RPSS) measures cumulative squared error between categorical forecast probabilities and the observed categorical probabilities relative to a reference (or standard baseline) forecast. When using the terciles computed from observation climatology (CHIRPS precipitation over the same period) RPSS informs if the forecasts are better than simple climatology.

RPSS for a collection of RPS values relative to the RPS computed from the climatological probabilities can be derived as:

$$RPSS = 1 - \frac{< RPS >}{< RPS_{Clim} >}$$

where $<\cdot>$ denotes average over forecasts. RPSS greater than zero indicates that the actual forecast outperforms the climatology. RPSS smaller or equal than zero indicates no skill as our forecast is less accurate than simple climatology. Skills are computed for the multi-system and for each forecasting system for internal check (not shown in the website) in the latitude band covered by CHIRPS (i.e. between 50° N and 50° S).

3.3. Mosaicking tercile maps to ASAP phenology

With tercile maps, forecasted rainfall for future time periods (e.g. next month, next two months, etc.) is classified into three categories: drier than normal, normal and wetter than normal, each one with an associated probability of occurrence. Although informative, such maps are difficult to be handled by an informed analysist and cannot be directly exploited by an automatic algorithm designed to trigger a warning in case of negative precipitation prospects. In fact, a tercile map provides a wall-to-wall spatial coverage of the most probable precipitation outcome in a reference period. That is, for a given time period, the tercile probability may identify anomalous rainfall conditions in a grid cell (e.g. drier than usual for the next month). However, such information may be irrelevant for crop development because either no crops are present in the cell or crops are present but the time period does not (or only partially does) coincide with the expected growing period. That is, the information that above or below normal precipitation is likely to occur, is of little interest for agriculture monitoring if the period to which it refers to is not agronomically relevant (i.e. it is well before sowing or after harvesting). It may be even misleading as communicating drier than usual conditions in a period of the year where precipitation is typically low and crops are not growing may raise a false alarm.

While directly feeding an automatic system directly with the fixed time-window tercile maps is clearly not possible, the informed analyst may undertake the challenging task of understanding where and when the information provided is agronomically relevant. While this task could be feasible for an expert analyst undertaking the analysis of a single area of interest with homogeneous timing of the growing season, it gets more complex when the area of interest is larger and includes regions with crops growing at different time of the year. In fact, the analysis of such an area would require identifying and analyzing multiple maps at the same time. Obviously, the task becomes quickly unfeasible for an anlysists undertaking the analysis of multiple countries for a global early warning system such as ASAP.

To better illustrate the complexity of the interplay between crop or rangeland seasonality and precipitation forecasts we take the example of the relatively small region of Juba Hoose in the south of Somalia analyzed in August. Fig. 2 shows the climatology of the 10-day cumulative precipitation and the percentage of total crop area where crops are in the growing period. The figure depicts a region with bimodal rainfall distribution (*Deyr* and *Gu* rain in April-June and November-December, respectively) and two growing seasons per solar year.

In such an area, inspecting the typical tercile map for the next three months (here August-September-October from the SCF issued in August) would be misleading for the agricultural analyst because no matter the precipitation probability category, rainfall is typically low and crops are being harvested in August to September.

This means that the analyst has to browse the tercile maps, each referring to a specific period, to select the relevant one for the specific area of interest. For the Somalia example and a time of analysis in August, the October-November-December would be the most informative on the subsequent growing season. This is indeed the current practice for this region where the MAM (March-April-May) and OND (October-November-December) periods are typically selected to approximate the two growing seasons.[6]

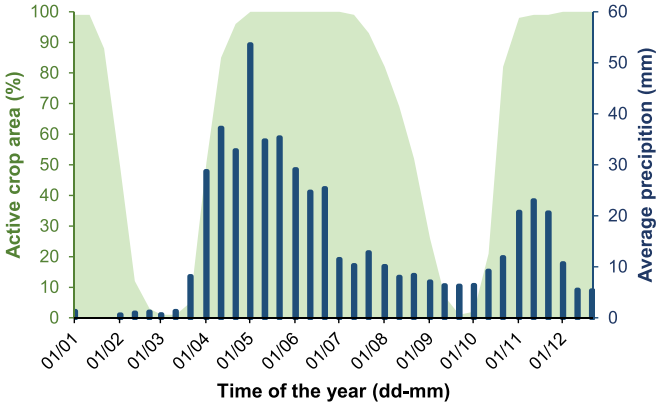

Fig. 2. Average 10-day cumulative precipitation from CHIRPS over cropland areas and percent of cropland area with growing crops in Juba Hoose administrative region in the south of Somalia.

[6] https://cropmonitor.org/documents/SPECIAL/reports/Special_Report_20220523_East_Africa.pdf.

Selecting a single reference period for an area of interest is not trivial either. Crop calendars are typically available at national level and may be used to identify the relevant agronomic period. However, crop phenology may vary within a country, adding an additional challenge to the analyst that should refer to multiple tercile maps when interested to analyze a large area. For example, according to ASAP phenology, the growing season of the region of Hiraan in central Somalia is anticipated of about one month as compared to Juba Hoose region.

This problem is not new to early warning decision support systems such as the JRC-ASAP (Meroni et al., 2019; Rembold et al., 2019). The system, analyzing remote sensing and gridded meteorological indicators, focuses on crop areas (or alternatively, rangeland areas) during the average growing season period in each grid cell to derive statistics of the various indicators and combine them into "warning" levels at some sub-national administrative level. Again hereafter we will drop reference to rangeland for conciseness. Anomalous conditions occurring in areas without crops or outside the average growing period are considered irrelevant for crop monitoring. Despite being an obvious simplification of the problem, it allows focusing the analysis on the right place and time.

To focus on the right place (where crops or rangeland are potentially growing at some time during the year), ASAP simply uses a static area fraction images at 1 km spatial resolution (Section 2.1). To focus on the right time (i.e. when crops are growing), ASAP uses the satellite-derived average growing season timings. Among the land surface phenology parameters described in Section 2.2, the time of start of season and the time of start of senescence period are available per grid cell for one or two growing season per solar year. Such land surface phenological events are expressed in dekads, nearly 10-day time periods (i.e. 36 dekads in a year, 3 in a month: day 1 to day 10, day 11 to 20, day 21 to end of the month). With this information it is then possible to determine at any time of the year (i.e. the time of analysis) if a pixel is "active" (i.e. in the period of average growing season). In the ASAP system, remote sensing and meteorological indicators are considered relevant only during this period.

While this is straightforward in a monitoring approach, it requires some specifications when analyzing precipitation in forecasting mode. In this case, the analyst is typically interested in the likely precipitation outcome during the remaining part of the current season (if the time of analysis falls within a growing season period in a given grid cell) or the next growing season otherwise (if there is no growing season at the time of analysis).

With the objective of providing such information, we adopt here the ASAP approach to extract the relevant information from the multiple tercile maps and "mosaic" it into a single map showing the most likely probability for the remaining part of the current season or the next one if there is no started season yet.

ASAP analyses various indicators including the biomass proxy (i.e. NDVI) during the entire growing season (from SOS to EOS) to compute warnings. However, precipitation data used to compute the warning levels does not fully coincide with such a period. In fact, precipitation information for crop monitoring starts to be relevant before the SOS, when crops are sown. This is accounted for in ASAP by considering the Standard Precipitation Index with a three months time scale (SPI3), therefore extending before SOS of the period considered. Similarly, a period before SOS is considered to initialize the soil water content used in the computation of the second water-related indicator, the Water Satisfaction Index (WSI, Boogaard et al., 2019). In addition, anomalies in precipitation-based indicators (SPI3 and WSI) are not considered relevant after the start of the senescence period (i.e. during the period from SEN to EOS) because plants are naturally drying out and the variability of precipitation is less relevant.

In a similar way, the appropriate period used for the analysis of precipitation forecasts is defined as follows. As satellite-based phenology SOS captures a time when vegetation is in an initial growth phase (Meroni et al., 2021a), extending backward in time the reference period can be useful to cover the period from sowing time to emergence of the crop. As sowing dates are not available, we pragmatically extend the reference period to one month before SOS and we denote this timing as SOW. Similarly to the definition used for SPI3 and WSI, we select SEN as the end time for the target period.

In order to avoid increasing the computational burden we round dekadal SOW and SEN values to monthly values to directly source tercile and skills maps computed as described in Section 3.1 and 3.2. In fact, using the dekadal time step would require computing tercile and skill maps starting from daily forecasts. The following rule is applied for rounding: if the period is overlapping with two or more dekads of the month, the month is included, it is excluded otherwise. The "season" period relevant for precipitation forecasts spans thus from SOWm to SENm, where m indicates the monthly time step.

SCF are issued on the 13th of each month. We denote as *cm* the current month, at which the analysis is performed. Precipitation forecasts cover a 6-month period from *cm* to *cm* + 5 (included). The computation of the phenology adjusted precipitation tercile map at the time of analysis thus proceeds as follows for each ASAP 1-km grid cell:

- In the case the cell has two seasons per year, we focus on SOWm and SENm of the closest one (the one being active or the first to come if no season is active);
- If SOWm starts before the current month (SOWm $<$ *cm*) then SOWm is moved to the current month (SOWm $=$ *cm*): IF SOWm $<$ *cm* THEN SOWm $=$ *cm*; i.e. the season already started, we focus on the part to come;
- If SENm falls after the period covered by the forecast (SENm $>$ cm + 5) then SENm is moved to the end of the forecast period (SENm $=$ cm + 5): IF SENm $>$ *cm* + 5 THEN SENm $=$ *cm* + 5; i.e. when the end of the season occurs beyond the SCF forecasting horizon we truncate the season;
- With updated SOWn and SENm by grid cell we select the corresponding tercile and skill maps (i.e. with reference period SOWn to SENm).

Given that in each 1-km grid cell we may select a different period for extracting the precipitation forecast, it follows that the skills of the phenology adjusted forecast map also vary by cell.

In order to provide the analyst with all the relevant information we produce the following mosaicked maps: tercile probability, skills, and a lead time map showing the number of dekads from the time of analysis to the start of the season of reference (i.e. SOW of the current season or the next one). The lead time map can have thus both negative and positive values, if the season has already started or if it is yet to start, respectively. We also produce two additional maps showing the percentage of the season that is still to be experienced (100 % if the season has not started yet, less than 100 % if the season is ongoing) and percentage of such period that is actually covered by SCF. A percentage smaller than 100 thus indicating the forecasting horizon does not fully cover the entire season of interest.

4. Results

4.1. Seasonal forecast tercile maps

Tercile maps referring to all monthly aggregations that can be formed with the forecasts are updated every month and published in the ASAP website[7] for global and continental windows (Supplementary Material Fig. S1 for an overview). Fig. 3 shows an example of the tercile

[7] https://mars.jrc.ec.europa.eu/asap/seasonal_forecast.php.

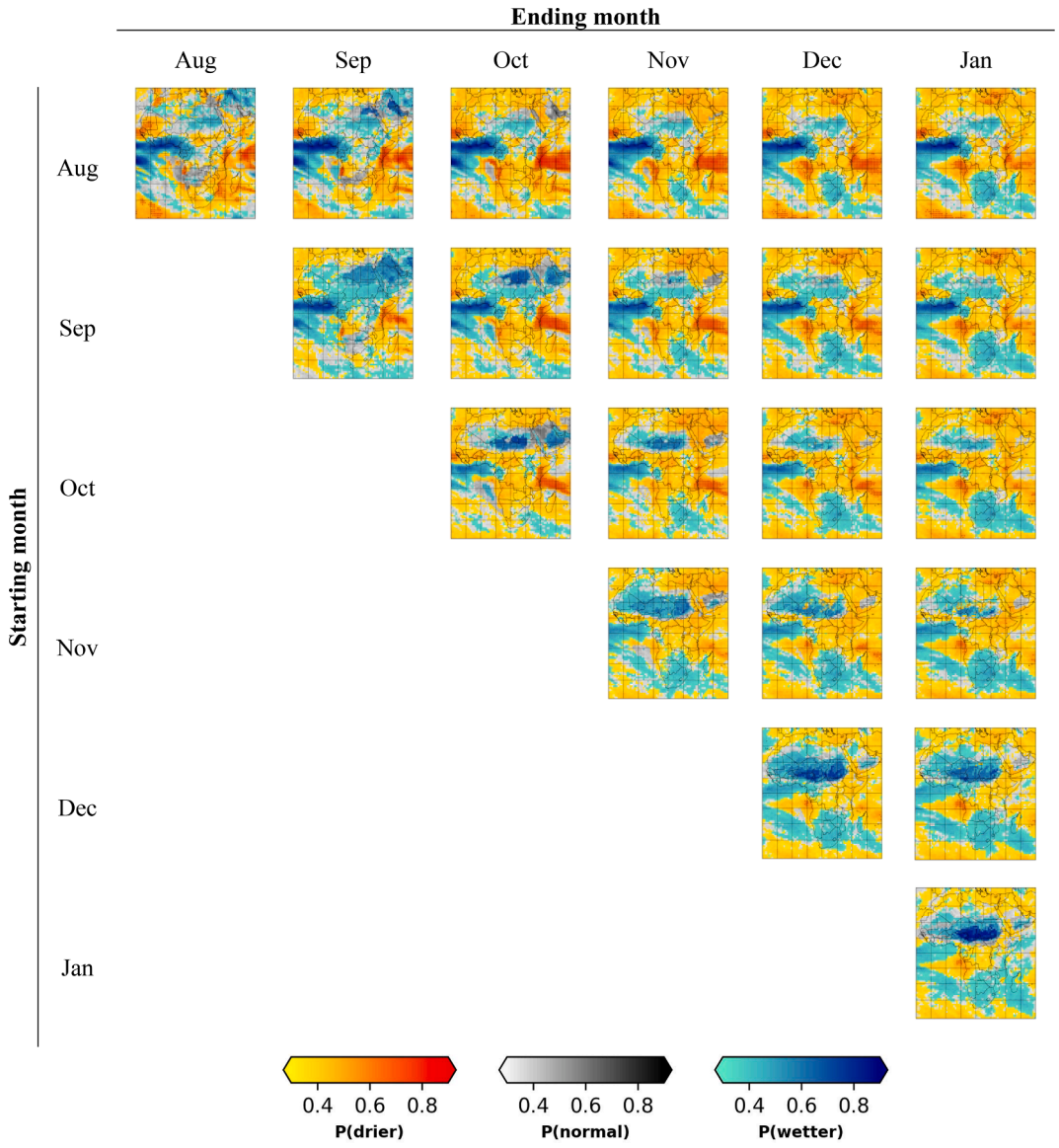

Fig. 3. Example of tercile maps over all possible monthly aggregations for the seasonal forecast of August 2021 referring to the forecast horizon 01/08/2021 – 31/01/2022. Rows and columns indicate the starting and ending month, respectively. The "+" sign indicated a relatively high probability (i.e. at least 32%) of precipitation equal or below the 16th percentile (that is below the standard deviation).

maps produced in August 2021 for the African continent.

Similar tercile maps can be obtained from the C3S multi-model ensemble from Copernicus web site[8] for the next three months while user defined periods can be requested to the interactive user interface to the WMO Lead Centre for Long-Range Forecast Multi-Model Ensemble.[9] Compared to such visualization tools, the proposed one has the advantage of offering a quick overview of all possible monthly time ranges and the possibility of inspecting the skill (see Section 3.2) by switching from forecasts to skill-view.

Nonetheless, Fig. 3 exemplifies the inherent challenges a user interested in agriculture may face in correctly interpreting the information provided by the tercile maps. As an example consider the inspection of a single map, e.g. that for the next three months, August to October (reported in Fig. 1 with larger format). Both positive and negative anomalies are present in the African continent, are they all agronomically relevant? They are not in North Africa, where cereals are sown in October-November. As harvesting takes place from May, the October to January (last month of the forecast horizon) may be more appropriate and informative for the initial development of the crops. They are not fully relevant in Somalia, where the growing season turns to an end in August and precipitation is typically low in September (see Fig. 2). Again, they are not appropriate in the east of South Africa, where austral summer crops are dominant and the growing season is between November and May, nor in the west of South Africa, where austral winter crops are dominant but the growing season is ending.

Let consider the work of an analyst tasked to monitor a specific country, e.g. South Africa. For explanatory purposes, assume that the analyst has no specific knowledge about the country. First, the analyst needs to retrieve information about the crop calendar to determine which map, if any of those available, should be inspected. Crop

[8] https://climate.copernicus.eu/charts/c3s_seasonal/c3s_seasonal_spatial_mm_rain_3m?facets=undefined&time=2022120100,744,2023010100&type=tsum&area=area08.

[9] https://www.wmolc.org/seasonPmmeUI/plot_PMME#.

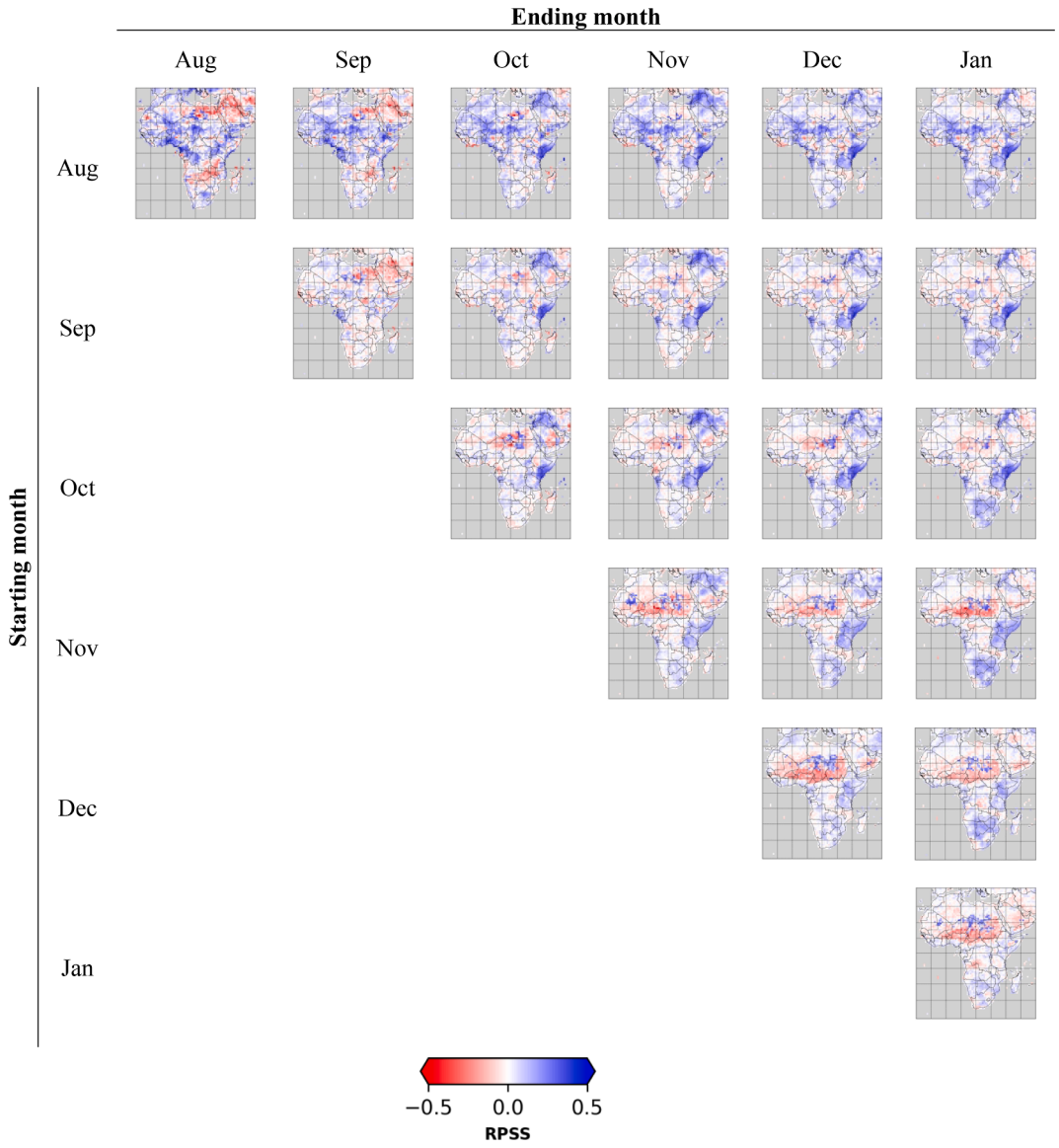

Fig. 4. Example of skill maps over all possible monthly aggregations for the seasonal forecast of August 2021 referring to the forecast horizon 01/08/2021 – 31/01/2022 (tercile maps in Fig. 3).

calendars are often available at the country level (e.g. FAO crop calendar[10]). Such national crop calendars show that both summer and winter crops are present and growing at different times. Additional information gathering would be thus needed to locate where they grow and thus finally come to the conclusion that for the eastern provinces, where summer crops are growing in the period November to July, the map November - January is offering the largest overlap with the growing season. On the contrary, for the western provinces where winter cereals are growing in the period May to October, none of the current maps offer useful information.

The same reasoning applies if instead of the analyst without specific knowledge about the area, we think of an algorithm supposed to issue warnings based on precipitation forecasts in a similar way as the warning classification scheme used by ASAP. The algorithm would need to have access to that ancillary information needed to determine when and where SCF are agronomically relevant, which is exactly the scope of this work.

[10] https://www.fao.org/giews/countrybrief/country.jsp?code=ZAF.

4.2. Skill

The skill of precipitation forecasts shown in Fig. 3 is reported in Fig. 4 (all dates available at https://agricultural-production-hotspots.ec.europa.eu/seasonal_forecast.php).

As expected the skill of single month predictions (maps along the diagonal in Fig. 4) tends to decrease with increasing lead time as observed by Gebrechorkos et al. (2022). This pattern is observable in Fig. 5 that depicts the decrease of the average skill at the global level by increasing lead time.

However, this climatological view hides some important information, e.g. the skill is not homogeneous by forecasting month. In fact, despite this decreasing trend, minimum and maximum skills (reported in Supplementary Figs. S2 and S3) highlight the variability in skill that can range from very low to quite high depending on the forecasting month. Taking Africa as an example, minimum skills for forecasts with 1 to 3 months lead time are reached towards the end / beginning of the calendar year in Western Africa and north of Central Africa (Supplementary Fig. S4). These lead times at such forecasting times correspond roughly to forecasts during the months from December to March, when the excursion of the Intertropical Convergence Zone (ITCZ) has not

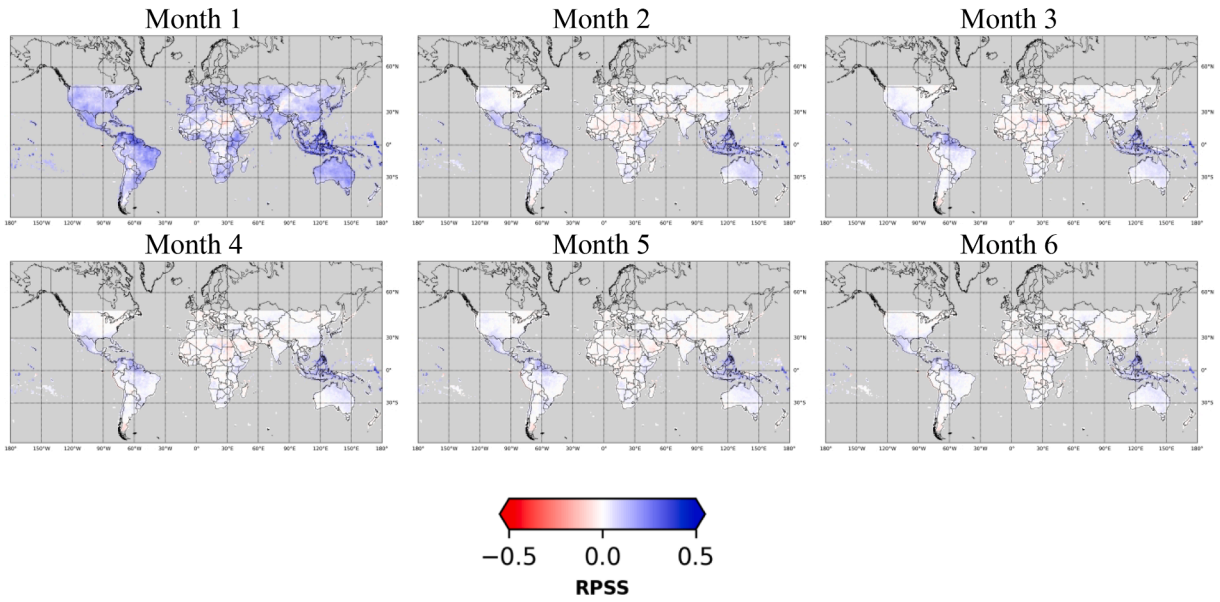

Fig. 5. Average RPSS by lead time, from one to six months. Average RPSS is computed over all forecasting dates (12 months) and hindcasting years.

reached the concerned area and precipitation is minimal according to CHIRPS climatology (Supplementary Fig. S6) and thus not relevant for agricultural monitoring. For lead times 4 to 6 in the same area, minima are found at forecasting times between May and August (Fig. S4). This corresponds again to the forecasts during months from December to March as discussed above.

Analogous reasoning can be applied to maximum skills (Supplementary Fig. S5). Highest skills for Somalia and lead times 1 to 3 can be found at forecasting times of August (for lead time 3) to October (for lead time 1), both pointing to the month of October where precipitation is maximum according to CHIRPS climatology (Supplementary Fig. S6). Interestingly, we note that this area is subjected to bi-modal precipitation distribution (short and long rainy seasons in October–November and April–June, respectively) and the SCF performs better during the short rainy season in agreement with Mwangi et al. (2014).

While SCF has obvious skill limitations, these roughly reflect the difficulties of modelling precipitation in dry periods (see e.g. Landman et al., 2012). However, such periods are not agronomically relevant and this observation points again to the fact that SCF should be tailored to the actual growing season period to deliver a more comprehensible information about precipitation and associated skills.

4.3. *Mosaicking tercile maps to ASAP phenology*

Left panels of Fig. 6 show the phenology adapted tercile map produced in August 2021 (compare with standard terciles maps of Fig. 3) for all vegetated grid cells (Fig. 6A, i.e. all areas exhibiting a seasonal vegetation cycle), cropland (Fig. 6B) and rangelands (Fig. 6C). Right panels of Fig. 6 shows the associated skill.

Fig. 7 shows the temporal details that complement the information provided by the phenology adapted tercile maps of Fig. 6. The first column shows the time to SOW; positive values indicate that the season has yet to start and thus the tercile value refers to an upcoming season while negative values indicate that the season has already started and thus the tercile value refers to an ongoing season (started but not concluded). The second column shows the percentage of the season remaining. Upcoming seasons thus have 100 % remaining while ongoing seasons can have variable percentages according to their progress. The third and last column shows to what extent the remaining part of an ongoing season (or the full period of an upcoming one) is covered by the precipitation forecast.

To discuss the resulting phenology adapted tercile map, we focus on the following regions: Northwest Africa, the Horn of Africa, and South Africa. The time of analysis refers to the first of August 2021, starting period of the seasonal climate forecasts covering the period August 2021 – January 2022.

In Northwest Africa (e.g. Morocco, Algeria, Tunisia) there is no active growing season occurring at this time. The following crop season starts in November as shown in the time to SOW map of Fig. 7 with values between 8 and 10 dekads. Since the season has yet to come, the percentage of remaining season is 100 % (see % of season remaining of Fig. 7). Senescence occurs in this region around April, well beyond the period covered by the forecast. Thus, the percentage of the target season that is covered by the forecasts ranges from 30 to 50 % (see % of remaining season covered by SCF of Fig. 7). The tercile map of Fig. 6 shows that for the part of the coming season that is covered by SCF (roughly the period November to January), a drier than normal precipitation is forecasted. However, the temporal intersection between the growing season period and the SCF forecast horizon selects the last three months in the forecasting horizon, where skill tends to degrade (Fig. 5). As a result, skills for this area at this time of analysis are low (see RPSS of Fig. 6).

In the Horn of Africa, drier than normal conditions are forecasted for most of the bimodal areas (i.e. having two growing seasons per year) of the region: South East of Ethiopia, Somalia, and Kenya. This affects both cropland and rangeland areas, the latter covering most of the land in the south of Ethiopia, Somalia and northern Kenya. The season in the bimodal areas starts after one to two months depending on the locations as shown by time to SOW of 3 to 6 dekads and the percentage of remaining season of 100 %. The upcoming season is the short rainy season, lasting only a few months in the area (see for example Fig. 2). The season can be fully covered by the SCF issued in August as shown in the percentage of remaining season covered by SCF, also 100 % for the bimodal areas. Phenology adapted skills are positive and thus provide an indication of reliability of the forecasts for the upcoming season. Retrospective analysis carried out at the time of writing shows that drier than usual conditions actually occurred in the period September 2021 to November 2021 (Supplementary material Fig. S7).

SCF in South Africa depicts different conditions in the West and East of the country. The West (i.e. Western Cape province and the western part of the Northern Cape province) receives most of the precipitation during the austral winter and winter cereals are typically grown roughly

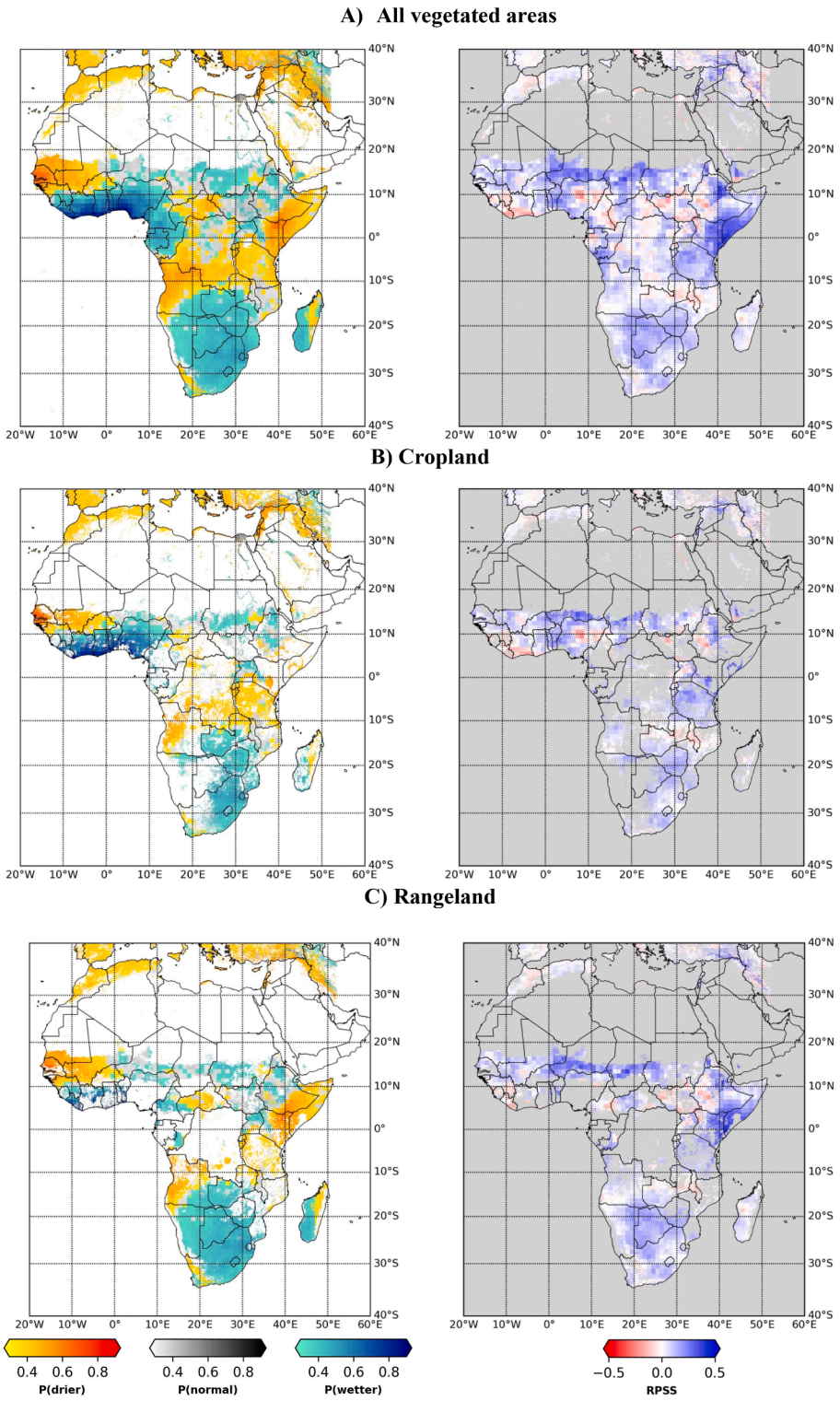

Fig. 6. Phenology adapted tercile maps for the seasonal forecast of August 2021 referring to the forecast period 01/08/2021 – 31/01/2022.

between March and September. On the contrary, the East of the country receives most of the precipitation during the austral summer and summer crops are grown between October and May (mostly maize, sunflowers, soybeans). This is fully reflected in the time to SOW map showing that the season has already started in the West (i.e. negative values) while it has yet to start in the East (i.e. positive values). Only about 20 % of the winter cereal season is left in the West while 100 % of the season is still to come for the summer crops in the West. By inspecting the map of percentage of the season that is covered by SCF over croplands we observe that, in agreement with local crop calendars, the remaining part of the season is fully covered in the West while roughly half of the upcoming season is covered in the East. Interestingly, it is possible to observe a latitudinal band roughly stretching north-west from Namibia to south-east in south Africa, separating the two climatic zones and mostly occupied by rangeland, where the percentage covered is smaller. The season in this transition band is longer because rain is

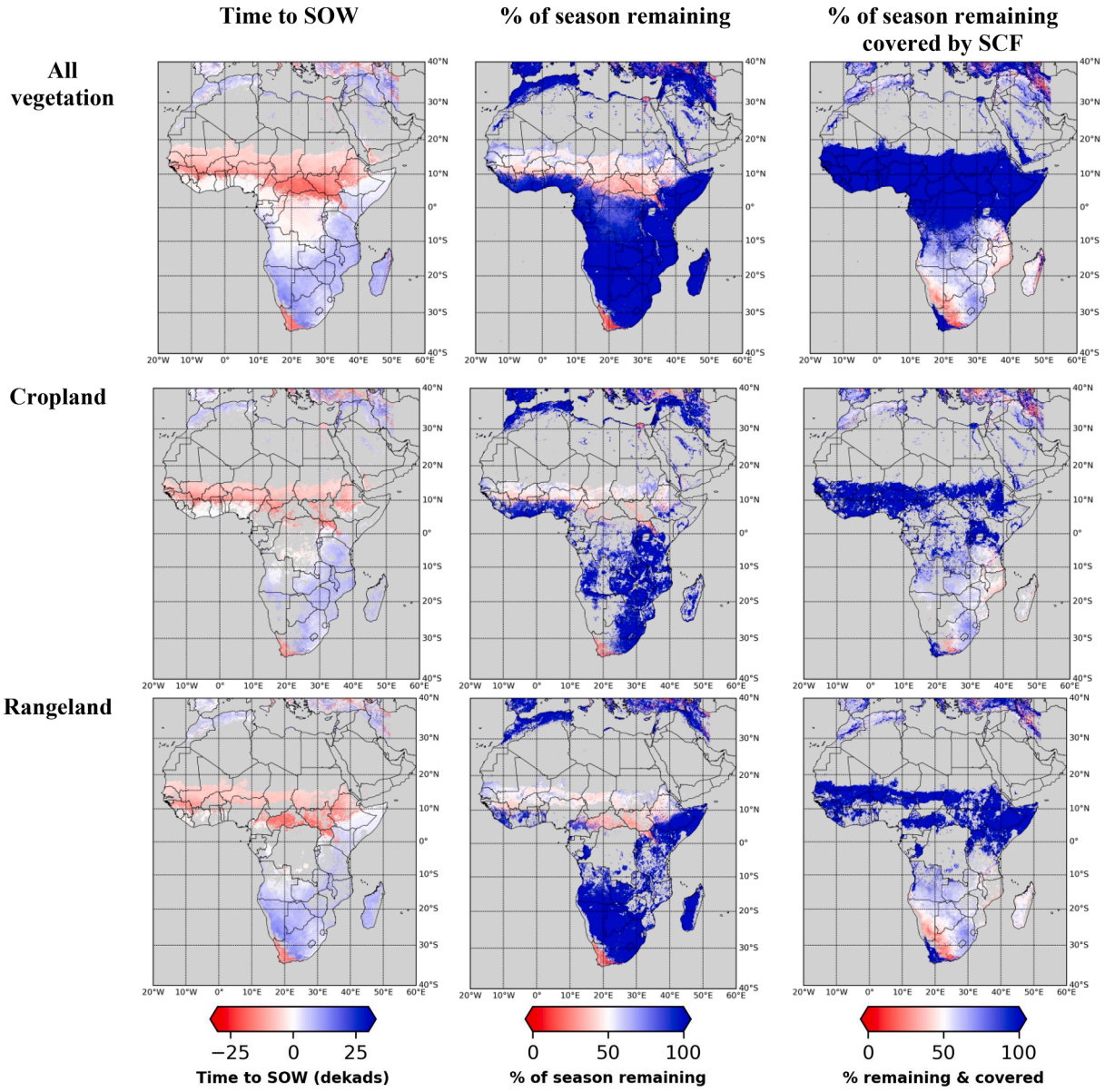

Fig. 7. Ancillary information related to the phenology adapted tercile map for the seasonal forecast of August 2021 referring to the forecast period 01/08/2021 – 31/01/2022.

more evenly distributed between winter and summer. The phenology adapted tercile map indicates drier than normal conditions in most of the western winter cereal region (with the exception of the coastal area around Cape Town where forecasts are normal or above normal). On the contrary, wetter than normal conditions are forecasted for rangeland band mentioned above and the western summer crop area. Skills are positive and, interestingly, similar for the whole country despite they refer to quite different periods, i.e. a closer one for the West and a later one for the East. Retrospective analysis on CHIRPS data confirms drier than normal conditions occurred in the west for the remaining part of the season (i.e. roughly the month of September, Supplementary material Fig. S8, note that also the normal conditions around Cape Town are confirmed) while normal to wetter than normal conditions were observed in three months of 2021 (Supplementary material Fig. S9).

5. Discussion

As a first step for tailoring precipitation SCF to agriculture monitoring, we produced tercile maps and skill maps for all the possible aggregation periods within the forecasting lead-time (Fig. 3). This visualization adds information with respect to the seasonal forecast precipitation charts released directly by Copernicus C3S over the three-month accumulation window following the forecast release. Apart from highlighting the very likely drought-prone areas (i.e., the + sign used in the maps), it is possible to select the most suitable time-horizon for targeted applications. In fact, the three-month interval is not the only visualized, but all temporal aggregations from a month to six months are also available.

After that, we overcome the difficulties an analyst might face in selecting the relevant time horizon per area of interest by integrating the tercile maps with climatological satellite phenology. With this approach it is possible to mosaic only relevant information from the tercile maps and show the probability of the most likely tercile for the closest agricultural season (i.e. the current one, if any, or the next one). In this way, the analyst is presented with information regarding the probability of precipitation for the relevant agronomic period, changing by location and broad agronomic types (i.e. cropland and rangeland). Ancillary information, including the timing of the season targeted, the coverage

offered by SCF and their skills, are provided.

Besides facilitating the expert-based qualitative analysis, this set of information represents the building block of an automatic quantitative analysis that will be included into the ASAP system. The system is currently focused on monitoring agriculture during the growing season and triggering automatic warnings at the first to second sub-national administrative level driven by observed anomalies of various environmental indicators. ASAP will be thus complemented by a warning on future precipitation when the phenological adapted tercile map indicates below normal conditions for the remaining part of the season or the upcoming one. Together with information about the outcome of the last consecutive growing seasons, this view on the upcoming one is of critical importance for food security analysis and response planning.

Additional use of the phenology integrated precipitation forecasts is foreseen in the crop yield forecasting domain. Yield forecasting typically builds on establishing a relation between environmental and climatic drivers (e.g. precipitation, temperature, biomass status) observed during the growing season and the final yield (Basso and Liu, 2019; Schauberger et al., 2020).

While the observed state of the agricultural system from the start of the growing season up to its end is clearly informative of the final yield, it has typically poor predictive power at the initial stages of season, i.e. the accuracy of the predicted yield increases along the growing season when more and more information becomes available (e.g. Meroni et al., 2021b).

Iizumi et al. (2018) used seasonal temperature and precipitation forecasts derived from a multi-model ensemble for forecasting crop yield at the global level. The relevant agronomic period was selected using global crop calendars and focusing on a 3-month interval just before harvesting, representing a simplification of the reproductive growth period. Information derived from SCF and tailored to the phenology of the area of interest may thus be used to improve crop yield forecasts.

6. Conclusions

We propose an effective method to quantify and efficiently communicate seasonal precipitation forecasts focused on agriculture monitoring. We tailored Copernicus C3S /multi-model seasonal forecast ensemble data to crop and rangeland phenology to extract only the agronomically relevant information.

In this new forecast products, seasonal precipitation are tailored to match the temporal dynamics of crops and rangeland using the remote sensing derived Land Surface Phenology information at 1 km spatial resolution. Precipitation forecast for the relevant agronomic period are mosaicked globally to derive precipitation probability maps that inform the user on the likely precipitation for the remaining part of the agricultural season (where a season is ongoing at the time of analysis) or for the upcoming season (where the timing of analysis falls between the seasons). This information, together with its reliability from mosaicked skill information, provides a direct overview of the precipitation probability relevant to agriculture and can be ingested in the automatic processing of early warning systems such as ASAP to trigger warnings of future precipitation deficit.

The implementation of the visualization of the phenology adapted precipitation tercile maps, together with their use in the ASAP warning system, is currently underway. This will add a forecasting component to the existing monitoring platform. During the growing season, the system will be complemented by warning prospects based on precipitation forecasts for the remaining part of the season using the current ASAP logic, i.e. if more than 25 % of the agricultural (or rangeland) area is affected by negative anomalies, in this case higher probability for the lowest tercile. Similarly, in between two seasons, when the current monitoring system is not active, ASAP will trigger warnings concerning the next season to come. A further next step will regard the production of the phenology adapted tercile maps for temperature that, together with precipitation, represents a main driver of drought by augmenting the evaporative demand and thus leading to reduced water availability to plants with equal rainfall.

CRediT authorship contribution statement

Michele Meroni: Conceptualization, Data curation, Formal analysis, Investigation, Methodology, Software, Supervision, Writing – original draft, Writing – review & editing. **Petar Vojnović:** Formal analysis, Methodology, Software, Writing – review & editing. **Matteo Zampieri:** Conceptualization, Software, Writing – review & editing. **Stefano Materia:** Conceptualization, Writing – original draft. **Felix Rembold:** Conceptualization, Project administration, Supervision, Writing – original draft, Writing – review & editing. **Oliver Kipkogei:** Conceptualization, Writing – review & editing. **Andrea Toreti:** Conceptualization, Writing – review & editing.

Declaration of competing interest

The authors declare that they have no known competing financial interests or personal relationships that could have appeared to influence the work reported in this paper.

Data availability

Data will be made available on request.

Acknowledgements

This work has been supported by the FOCUS-Africa Horizon 2020 project (grant agreement No 869575). The developed code can be obtained through direct request to the JRC authors.

Appendix A. Supplementary data

Supplementary data to this article can be found online at https://doi.org/10.1016/j.cliser.2023.100434.

References

Barnston, A.G., van den Dool, H.M., Zebiak, S.E., Barnett, T.P., Ji, M., Rodenhuis, D.R., Cane, M.A., Leetmaa, A., Graham, N.E., Ropelewski, C.R., Kousky, V.E., O'Lenic, E. A., Livezey, R.E., 1994. Long-lead seasonal forecasts—where do we stand? Bull. Am. Meteorol. Soc. 75 (11), 2097–2114.

Basso, B., Liu, L., 2019. Seasonal crop yield forecast: Methods, applications, and accuracies, 1st ed, Advances in Agronomy. Elsevier Inc. doi: 10.1016/bs.agron.2018.11.002.

Becker-Reshef, I., Justice, C., Barker, B., Humber, M., Rembold, F., Bonifacio, R., Zappacosta, M., Budde, M., Magadzire, T., Shitote, C., Pound, J., Constantino, A., Nakalembe, C., Mwangi, K., Sobue, S., Newby, T., Whitcraft, A., Jarvis, I., Verdin, J., 2020. Strengthening agricultural decisions in countries at risk of food insecurity: The GEOGLAM Crop Monitor for Early Warning. Remote Sens. Environ. 237, 111553 https://doi.org/10.1016/j.rse.2019.111553.

Boogaard, H., van der Wijngaart, R., van Kraalingen, D., Meroni, M., Rembold, F., 2018. ASAP Water Satisfaction Index. Luxembourg. doi: 10.2760/478822.

Boogaard, H., Van Der Wijngaart, R., Kraalingen, V., Rembold, M., 2019. ASAP Water Satisfaction Index Technical Manual of WSI version 2.0, JRC Technical Reports. Luxembourg. doi: 10.2760/478822.

Chen, C.-T., Knutson, T., 2008. On the Verification and Comparison of Extreme Rainfall Indices from Climate Models. J. Clim. 21, 1605–1621. https://doi.org/10.1175/2007JCLI1494.1.

Crochemore L., Materia S., Delpiazzo E., et al., 2023 (submitted). Joint verification and evaluation of seasonal forecasts to enhance climate service uptake across multiple economic sectors. Bulletin of the American Meteorological Society.

De Beurs, K.M., Henebry, G.M., 2005. A statistical framework for the analysis of long image time series. Int. J. Remote Sens. 26, 1551–1573. https://doi.org/10.1080/01431160512331326657.

FAO, IFAD, UNICEF, WFP, WHO, 2018. The State of Food Security and Nutrition in the World. Building climate resilience for food security and nutrition. FAO, Rome.

FAO, IFAD, UNICEF, WFP, WHO, 2021. The State of Food Security and Nutrition in the World. Transforming food systems for food security, improved nutrition and affordable healthy diets for all. FAO.

Food Security Information Network et al., 2022. Global Report On Food Crisis 2022.

Fritz, S., See, L., Bayas, J.C.L., Waldner, F., Jacques, D., Becker-Reshef, I., Whitcraft, A., Baruth, B., Bonifacio, R., Crutchfield, J., Rembold, F., Rojas, O., Schucknecht, A.,

Van der Velde, M., Verdin, J., Wu, B., Yan, N., You, L., Gilliams, S., Mücher, S., Tetrault, R., Moorthy, I., McCallum, I., 2019. A comparison of global agricultural monitoring systems and current gaps. Agric. Syst. 168, 258–272. https://doi.org/10.1016/j.agsy.2018.05.010.

Funk, C., Peterson, P., Landsfeld, M., Pedreros, D., Verdin, J., Shukla, S., Husak, G., Rowland, J., Harrison, L., Hoell, A., Michaelsen, J., 2015. The climate hazards infrared precipitation with stations—a new environmental record for monitoring extremes. Sci. Data 2, 150066. https://doi.org/10.1038/sdata.2015.66.

Gebrechorkos, S.H., Pan, M., Beck, H.E., Sheffield, J., 2022. Performance of State-of-the-Art C3S European Seasonal Climate Forecast.pdf. Water Resour. Res. 1–18. doi: https://doi. org/10.1029/2021WR031480.

Giuliani, G., Nativi, S., Obregon, A., Beniston, M., Lehmann, A., 2017. Spatially enabling the Global Framework for Climate Services : Reviewing geospatial solutions to effi ciently share and integrate climate data & information. Clim. Serv. 8, 44–58. https://doi.org/10.1016/j.cliser.2017.08.003.

Hargreaves, J.C., 2010. Skill and uncertainty in climate models. WIREs Clim. Change 1, 556–564. https://doi.org/10.1002/wcc.58.

Hemri, S., Bhend, J., Liniger, M.A., Manzanas, R., Siegrt, S., Stephenson, D.B., Gutierrez, J.M., Brookshaw, A., Doblas-Reyes, F.J., 2020. How to create an operational multi-model of seasonal forecasts? Clim. Dyn. 55, 1141–1157. https://doi.org/10.1007/s00382-020-05314-2.

ICPAC, FAO, FEWS NET, WFP, EC-JRC, 2022. Unprecedented drought brings threat of starvation to millions in Ethiopia, Kenya, and Somalia. https://fews.net/sites/default/files/Joint%20Statement%20Horn%20of%20Africa%209%20June%202022.pdf, last accessed: 17/02/2023.

Iizumi, T., Shin, Y., Kim, W., Kim, M., Choi, J., 2018. Global crop yield forecasting using seasonal climate information from a multi-model ensemble. Clim. Serv. 11, 13–23. https://doi.org/10.1016/j.cliser.2018.06.003.

IPCC, 2021. Climate Change 2021: The Physical Science Basis. Contribution of Working Group I to the Sixth Assessment Report of the Intergovernmental Panel on Climate Change [Masson-Delmotte, V., P. Zhai, A. Pirani, S.L. Connors, C. Péan, S. Berger, N. Caud, Y. Chen, L. Goldfarb, M.I. Gomis, M. Huang, K. Leitzell, E. Lonnoy, J.B.R., Matthews, T.K. Maycock, T. Waterfield, O. Yelekçi, R. Yu, and B. Zhou (eds.)]. Cambridge University Press, Cambridge, United Kingdom and New York, NY, USA, 2391 pp., doi:10.1017/9781009157896.

IPCC, 2022. Climate Change 2022: Impacts, Adaptation and Vulnerability, Working Group II contribution to the Sixth Assessment Report of the Intergovernamental Panel on Climate Change. Cambridge University Press, Cambridge, U.K. and New York, NY, U.S.A. doi: 10.1017/9781009325844.

Jones, P.W., 1999. First- and Second-Order Conservative Remapping Schemes for Grids in Spherical Coordinates. Mon. Weather Rev. 127, 2204–2210. https://doi.org/10.1175/1520-0493(1999)127<2204:FASOCR>2.0.CO;2.

Kharin, V.V., Merryfield, W.J., Boer, G.J., Lee, W.S., 2017. A postprocessing method for seasonal forecasts using temporally and spatially smoothed statistics. Mon. Weather Rev. 145 (9), 3545–3561.

Klisch, A., Atzberger, C., 2016. Operational drought monitoring in Kenya using MODIS NDVI time series. Remote Sens. 8 https://doi.org/10.3390/rs8040267.

Landman, W.A., DeWitt, D., Lee, D.E., Beraki, A., Lötter, D., 2012. Seasonal rainfall prediction skill over South Africa: one-versus two-tiered forecasting systems. Weather Forecast. 27 (2), 489–501.

Lenssen, N.J., Goddard, L., Mason, S., 2020. Seasonal forecast skill of ENSO teleconnection maps. Weather Forecast. 35 (6), 2387–2406.

MacLeod, D., 2019. Seasonal forecasts of the East African long rains: insight from atmospheric relaxation experiments. Clim. Dyn. 53 (7–8), 4505–4520.

Materia, S., Muñoz, Á.G., Álvarez-Castro, M.C., Mason, S.J., Vitart, F., Gualdi, S., 2020. Multimodel subseasonal forecasts of spring cold spells: Potential value for the hazelnut agribusiness. Weather Forecast. 35 (1), 237–254.

Meroni, M., Rembold, F., Urbano, F., Csak, G., Lemoine, G., Kerdiles, H., 2019. The warning classification scheme of ASAP – Anomaly hot Spots of Agricultural Production, v4.0, JRC Technical Report. doi: 10.2760/798528.

Meroni, M., Vrieling, A., Fasbender, D., Lemoine, G., Rembold, F., Seguini, L., Verhegghen, A., 2021a. Comparing land surface phenology of major European crops as derived from SAR and multispectral data of Sentinel-1 and -2. Remote Sens. Environ. 253 https://doi.org/10.1016/j.rse.2020.112232.

Meroni, M., Waldner, F., Seguini, L., Rembold, F., 2021b. Agricultural and Forest Meteorology Yield forecasting with machine learning and small data : What gains for grains ? Agric. Meteorol. 308–309, 1–13. https://doi.org/10.1016/j.agrformet.2021.108555.

Mishra, N., Prodhomme, C., Guemas, V., 2019. Multi-model skill assessment of seasonal temperature and precipitation forecasts over Europe. Clim. Dyn. 52, 4207–4225. https://doi.org/10.1007/s00382-018-4404-z.

Mwangi, E., Wetterhall, F., Dutra, E., Di Giuseppe, F., Pappenberger, F., 2014. Forecasting droughts in East Africa. Hydrol. Earth Syst. Sci. 18, 611–620. https://doi.org/10.5194/hess-18-611-2014.

Nakalembe, C., Becker-reshef, I., Bonifacio, R., Hu, G., Laurence, M., Jade, C., Keniston, J., Mwangi, K., Rembold, F., Shukla, S., Urbano, F., Kathleen, A., Li, Y., Zappacosta, M., Jarvis, I., Sanchez, A., 2021. A review of satellite-based global agricultural monitoring systems available for Africa. Glob. Food Sec. 29, 100543 https://doi.org/10.1016/j.gfs.2021.100543.

Pérez-Hoyos, A., Rembold, F., Kerdiles, H., Gallego, J., 2017. Comparison of global land cover datasets for cropland monitoring. Remote Sens. 9 https://doi.org/10.3390/rs9111118.

Pérez-Hoyos, A., Udías, A., Rembold, F., 2020. Integrating multiple land cover maps through a multi-criteria analysis to improve agricultural monitoring in Africa. Int. J. Appl. Earth Obs. Geoinf. 88, 102064 https://doi.org/10.1016/j.jag.2020.102064.

Rembold, F., Meroni, M., Urbano, F., Csak, G., Kerdiles, H., Perez-hoyos, A., Lemoine, G., Leo, O., Negre, T., 2019. ASAP : A new global early warning system to detect anomaly hot spots of agricultural production for food security analysis. Agric. Syst. 168, 247–257. https://doi.org/10.1016/j.agsy.2018.07.002.

Schauberger, B., Jägermeyr, J., Gornott, C., 2020. A systematic review of local to regional yield forecasting approaches and frequently used data resources. Eur. J. Agron. 120, 126153 https://doi.org/10.1016/j.eja.2020.126153.

White, M.A., Thornton, P.E., Running, S.W., 1997. A continental phenology model for monitoring vegetation responses to interannual climatic variability. Global Biogeochem. Cycles 11, 217–234. https://doi.org/10.1029/97GB00330.

Wilks, D.S., 2011. Statistical Methods in the Atmospheric Sciences, Vol. 100. Academic press.

World Meteorological Organization, 2022a. State of the Global Climate 2021. Switzerland, Geneva.

World Meteorological Organization, 2022b. Provisional State of the Global Climate in 2022. Switzerland, Geneva.

World Meteorological Organization, 2012. Standardized Precipitation Index User Guide. World Meteorological Organization (WMO), Geneva, Switzerland.